Applied Mathematics & Information Sciences
An International Journal

http://dx.doi.org/10.18576/amis/180120

Stability and Hopf Bifurcation Analysis of a Fractional-Order Nicholson Equation with Two Different Delays

H. A. A. El-Saka[1,*], *D. El. A. El-Sherbeny*[1] *and A. M. A. El-Sayed*[2]

[1] Mathematics Department, Faculty of Science, Damietta University, New Damietta, 34517, Egypt
[2] Faculty of Science, Alexandria University, Alexandria, 21526, Egypt

Received: 12 Nov. 2023, Revised: 18 Dec. 2023, Accepted: 22 Dec. 2023
Published online: 1 Jan. 2024

Abstract: In this paper, we investigate the stability and Hopf bifurcation of fractional-order Nicholson equation with two different delays $r_1, r_2 > 0$: $D^{\alpha}y(t) = -\mu y(t-r_1) + \rho y(t-r_2)e^{-\gamma y(t-r_2)}$, $t > 0$. We obtain stability regions by analyzing the characteristic equation of the linearized model around the equilibrium points. We evaluate the effects of ρ and μ on the equilibrium point, which influence the model's stability and Hopf bifurcation. By choosing μ, ρ, fractional order α and time delays as a bifurcation parameters, the delay bifurcation curve for the emergence of the Hopf bifurcation is determined. Finally, numerical simulations are presented to illustrate the efficiency and validity of our results.

Keywords: Nicholson equation; Fractional differential equation; Time delays; Stability analysis; Hop bifurcation; Numerical solutions.

1 Introduction

Fractional calculus is becoming more important fields because of its applications in science and engineering [1, 2,3,4,5,6,7]. Delay differential equations (DDEs) are differential equations in which the derivative of a function at each given time depends on the solution at a previous time. DDEs have been used for analysis and forecasting in a wide range of life sciences fields, especially control systems, epidemiology, population dynamics, neutral networks, and physiology [3,8,9,10,11,12,13,14]. DDEs with two or more delays have attracted more interest recently [15,16]. The fractional delay differential equation (FDDE) has been used for several years in a number of fields, including economics, chaos, physics, control theory, agriculture, chemistry, neural networks, and bioengineering [5,17,18,19,20,21,22,23].

Fractional-delay differential equations have been studied by many researchers [24,25,26,27,28]. E. Ahmed et al. [26] studied the stability analysis of fractional-order predator-prey and rabies models and proved the existence, uniqueness of the solutions of the two models. El-Sayed et al. [27] analysed the existence and uniqueness of fractional-order logistic equations with two different delays. In 1980, Gurrney et al. [29] proposed the nonlinear differential equation of the form $\dot{N}(t) = -\delta + pN(t-\tau)e^{-aN(t-\tau)}$ to describe the population dynamics of Nicholson's blowflies. Where $N(t)$ is the size of population at time t, p is the maximum per capita daily egg production rate, $\frac{1}{a}$ is the size at which the population reproduces at its maximum rate, δ is the pair capita adult death rate and τ is the generation time. El-Sayed et al. [30] studied the stability of the equilibrium point of the fractional-order Nicholson equation. Faria and Henrique [31] analysed a Nicholson equation with multiple pairs of the varying delays and nonlinear terms given by mixed monotone functions. L. Yuying and J. Wei [32] investigated bifurcation analysis in the delayed Nichloson blowflies equation with delayed harvest. S. Panigrahi and S. Chand [33] used a fractional-order model with a time delay to discuss red blood cell survival in animals. Many researchers have proposed different types of fractional order time delay biological models and studied it [34,35].

In this paper, we analyse the stability and Hopf bifurcation of fractional-order Nicholson equation with two different delays using the critical curves method [11]:

* Corresponding author e-mail: halaelsaka@yahoo.com

$D^{\alpha}y(t) = -\mu y(t-r_1) + \rho y(t-r_2)e^{-\gamma y(t-r_2)}$, where D^{α} is a Caputo fractional derivative of order $0 < \alpha \leq 1$ and r_1, $r_2 > 0$. In Sec. 2, we obtained the stability analysis in two cases: $r_1 = r_2 = r$ and $r_1 \neq r_2$. The numerical simulations are presented in Sec. 3.

Definition 1.1. The Riemann-Liouville fractional integral operator of order $\alpha \in R^{+}$ of the function $f(t)$, $t > a$ is defined by

$$I_a^{\alpha} f(t) = \frac{1}{\Gamma(\alpha)} \int_a^t (t-\tau)^{\alpha-1} f(\tau) d\tau.$$

and the Caputo fractional derivative for $\alpha > 0$ of $f(t), t > a$ is defined by

$$D_a^{\alpha} f(t) = I^{n-\alpha} D^n f(t).$$

where $D = \frac{d}{dt}$, $\Gamma(.)$ is the Gamma function and $n-1 < \alpha \leq n, n \in N$.

For properties of fractional calculus see [1,36,37,38].

2 Main Problem and Dynamic Analysis

A fractional-order Nicholson equation with two different delays $r_1, r_2 > 0$ is

$$D^{\alpha}y(t) = -\mu y(t-r_1) + \rho y(t-r_2)e^{-\gamma y(t-r_2)}, \quad t \geq 0, \quad (1)$$

$$y(t) = \phi(t), \quad -\tau \leq t \leq 0. \quad (2)$$

where μ, ρ and γ are positive constant. D^{α} is a Caputo fractional derivative of order $0 < \alpha \leq 1$, the initial condition $\phi(t)$ is continuous on $[-\tau, 0]$ and $\tau = max\{r_1, r_2\}$.

The model (1) have two equilibrium points

$$y_1^* = 0, \quad (3)$$

and

$$y_2^* = -\frac{log\left(\frac{\mu}{\rho}\right)}{\gamma} > 0, \quad \text{if } \rho > \mu. \quad (4)$$

The stability analysis and Hopf bifurcation of the model (1) will be evaluated.

2.1 *Case 1: Dynamic analysis for one delay*

Let $r_1 = r_2 = r$ and $f(y(t-r)) = y(t-r)e^{-\gamma y(t-r)}$. Eq. (1) becomes

$$D^{\alpha}y(t) = -\mu y(t-r) + \rho f(y(t-r)), \quad (5)$$

and an equilibrium point y^* of Eq. (5) satisfy

$$-\mu y^* + \rho f(y^*) = 0. \quad (6)$$

Linearization about equilibrium

Let $\varepsilon = y - y^*$ be a small perturbation from an equilibrium point, $y_r = y(t-r)$ and $\varepsilon_r = \varepsilon(t-r)$. Then Eq. (5) becomes

$$D^{\alpha}\varepsilon = -\mu(\varepsilon_r + y^*) + \rho f(\varepsilon_r + y^*). \quad (7)$$

Then using Taylor's expansion, we get

$$D^{\alpha}\varepsilon = -\mu\varepsilon_r + \rho f'(y^*)\varepsilon_r, \quad (8)$$

Using Laplace transform Eq. (8) yields a characteristic equation

$$\lambda^{\alpha} + \left[\mu - \rho f'(y^*)\right] e^{-\lambda r} = 0. \quad (9)$$

Stability condition

An equilibrium point y^* is asymptotically stable if all the roots λ_i of the characteristic equation (9) satisfy

$$Re(\lambda_i) < 0. \quad (10)$$

When $r = 0$, the condition (10) is

$$\rho f'(y^*) - \mu < 0. \quad (11)$$

Now, let $r > 0$ and $\lambda = u + iv$, $u, v \in R$. A change in stability can occur only when the value of λ crosses the imaginary axis at $\lambda = iv$ and the characteristic equation becomes

$$(iv)^{\alpha} + \left[\mu - \rho f'(y^*)\right] e^{-ivr} = 0. \quad (12)$$

Separating real and imaginary parts of the Eq. (12), we obtain

$$v^{\alpha} cos\left(\frac{\alpha\pi}{2}\right) = -\left[\mu - \rho f'(y^*)\right] cos(vr), \quad (13)$$

$$v^{\alpha} sin\left(\frac{\alpha\pi}{2}\right) = \left[\mu - \rho f'(y^*)\right] sin(vr). \quad (14)$$

Squaring and adding Eqs. (13) and (14), we get

$$v^{2\alpha} = \left(\mu - \rho f'(y^*)\right)^2, \quad (15)$$

From Eq. (13), we get

$$r = \frac{1}{v}\left(2n\pi \pm arccos\left(\frac{v^{\alpha} cos\left(\frac{\alpha\pi}{2}\right)}{\rho f'(y^*) - \mu}\right)\right), n = 0, 1, \cdots. \quad (16)$$

Critical curves

The critical curves can be obtained by substituting from Eq. (15) in (16)

$$r_1(n) = \frac{2n\pi + arccos\left[\frac{\left(\mu - \rho f'(y^*)\right) cos\left(\frac{\alpha\pi}{2}\right)}{\rho f'(y^*) - \mu}\right]}{\left(\mu - \rho f'(y^*)\right)^{\frac{1}{\alpha}}}, \quad n = 0, 1, \cdots. \quad (17)$$

$$r_2(n) = \frac{2n\pi - arccos\left[\frac{(\mu-\rho f'(y^*))cos\left(\frac{\alpha\pi}{2}\right)}{\rho f'(y^*)-\mu}\right]}{(\mu-\rho f'(y^*))^{\frac{1}{\alpha}}}. \quad n = 1,2,\cdots. \tag{18}$$

Theorem 2.1. There is only one stability region for y^* located between $r = 0$ and the closest critical curve $r_1(0)$.

Proof. Differentiating the characteristic equation (9) with respect to r ($r > 0$), we get

$$\frac{d\lambda}{dr} = -\frac{\lambda^{\alpha+1}}{\alpha\lambda^{\alpha-1}+r\lambda^{\alpha}} \tag{19}$$

On critical curves (17) and (18),

$$\frac{du}{dr} = Re\left(\frac{d\lambda}{dr}\right)|_{\lambda=iv} = -\frac{z_1z_3+z_2z_4}{z_3^2+z_4^2}, \tag{20}$$

where

$$z_1 = v^{\alpha+1}cos\left(\frac{(\alpha+1)\pi}{2}\right),$$

$$z_2 = v^{\alpha+1}sin\left(\frac{(\alpha+1)\pi}{2}\right),$$

$$z_3 = \alpha v^{\alpha-1}cos\left(\frac{(\alpha-1)\pi}{2}\right) + rv^{\alpha}cos\left(\frac{\alpha\pi}{2}\right),$$

and

$$z_4 = \left(\alpha v^{\alpha-1}sin\left(\frac{(\alpha-1)\pi}{2}\right) + rv^{\alpha}sin\left(\frac{\alpha\pi}{2}\right)\right),$$

$$-(z_1z_3+z_2z_4) = \alpha v^{2\alpha} > 0. \tag{21}$$

Then

$$Re\left(\frac{d\lambda}{d\tau}\right)|_{\lambda=iv} > 0.$$

This implies that there does not exist any eigenvalue with negative real part across the critical curves (17) and (18). On the other hand, the equilibrium point y^* is asymptotically stable for $r = 0$. Thus, there is only one stability region enclosed by $r = 0$ and the critical curve $r_1(0)$, closest to it.

2.1.1 Stability for $y_1^* = 0$

From Eqs. (17) and (18), the critical curves for $y_1^* = 0$ are

$$r_1(n) = \frac{2n\pi+\pi(1-\alpha/2)}{(\mu-\rho)^{\frac{1}{\alpha}}}, \quad n = 0,1,\cdots. \tag{22}$$

and

$$r_2(n) = \frac{2n\pi-\pi(1-\alpha/2)}{(\mu-\rho)^{\frac{1}{\alpha}}}. \quad n = 1,2,\cdots. \tag{23}$$

We find that the critical curves are sensitive with the fractional order α, ρ and μ. See Fig. 1.

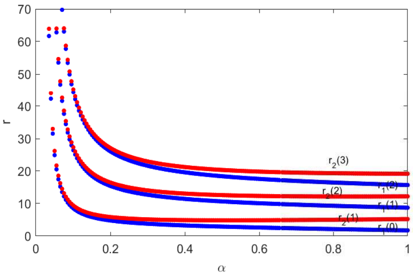

(a) $\rho = 0.1$, $\mu = 1$.

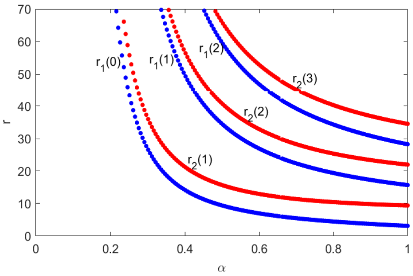

(b) $\rho = 0.5$, $\mu = 1$.

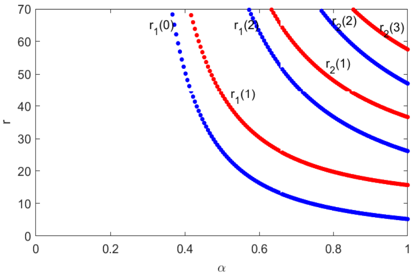

(c) $\rho = 0.7$, $\mu = 1$.

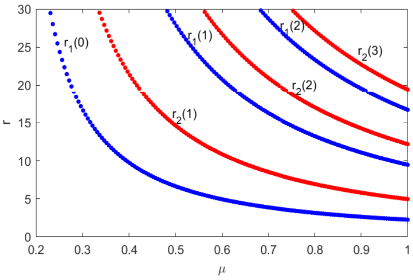

(d) $\alpha = 0.75$, $\rho = 0.1$.

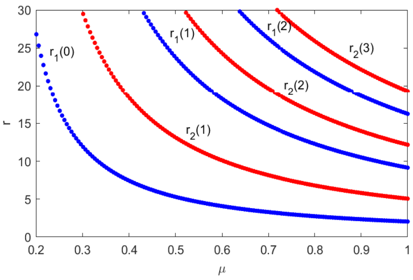

(e) $\alpha = 0.85$, $\rho = 0.1$.

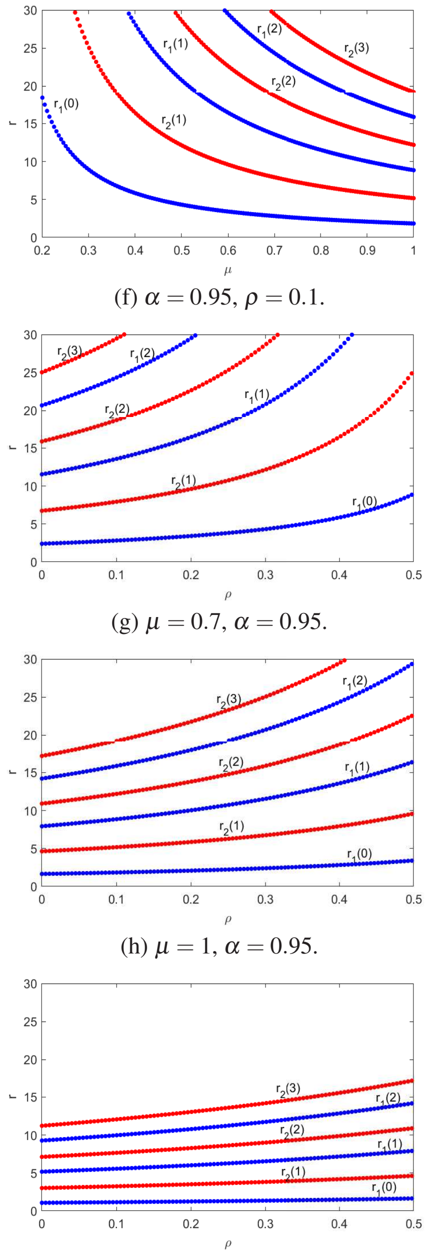

(f) $\alpha = 0.95$, $\rho = 0.1$.

(g) $\mu = 0.7$, $\alpha = 0.95$.

(h) $\mu = 1$, $\alpha = 0.95$.

(i) $\mu = 1.5$, $\alpha = 0.95$.

Fig. 1: Critical curves of Eqs. (22) and (23).

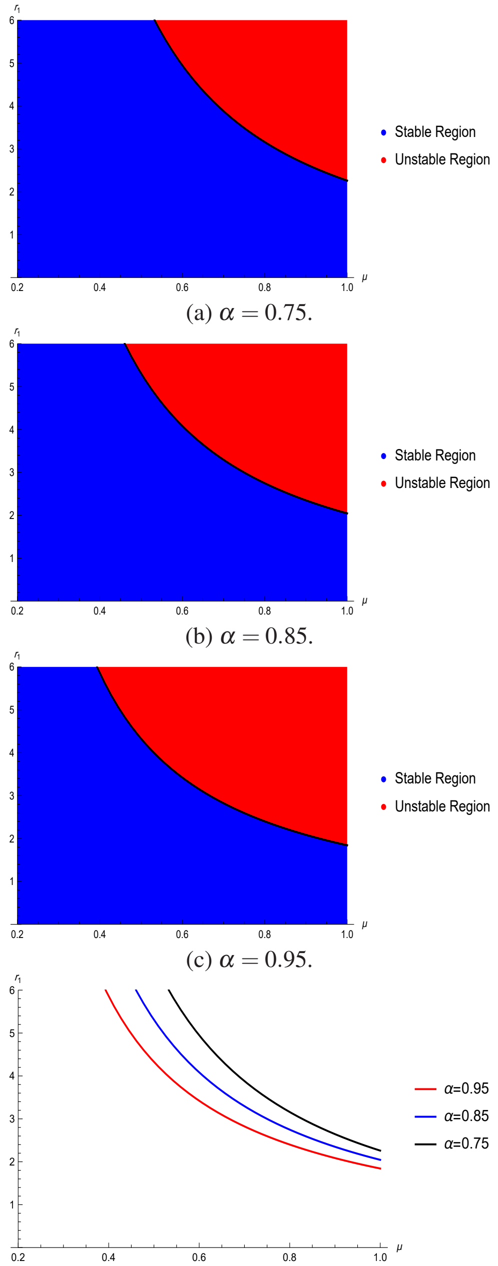

(a) $\alpha = 0.75$.

(b) $\alpha = 0.85$.

(c) $\alpha = 0.95$.

(d)

Fig. 2: Stability regions with respect to (μ, r_1) when α varies from 0.75 to 0.95 and $\rho = 0.1$.

Theorem 2.2. If $\rho < \mu$, then equilibrium point $y_1^* = 0$ of Eq. (5) has only stability region located between $r = 0$ and

$$r_1(0) = \frac{\pi(1-\alpha/2)}{(\mu-\rho)^{\frac{1}{\alpha}}}.$$

See Figs. 2-4. We observe that the stability regions are sensitive with the fractional order α, μ, ρ and time delay. Stability regions with respect to μ, ρ, α and time delay are given in Figs. 2-4 and critical surfaces in Fig. 5. Fig. 3 shows that stability domain increases as the value of ρ increases. Figs. 2 and 4 show that the stability domain increases as the values of α and μ decrease.

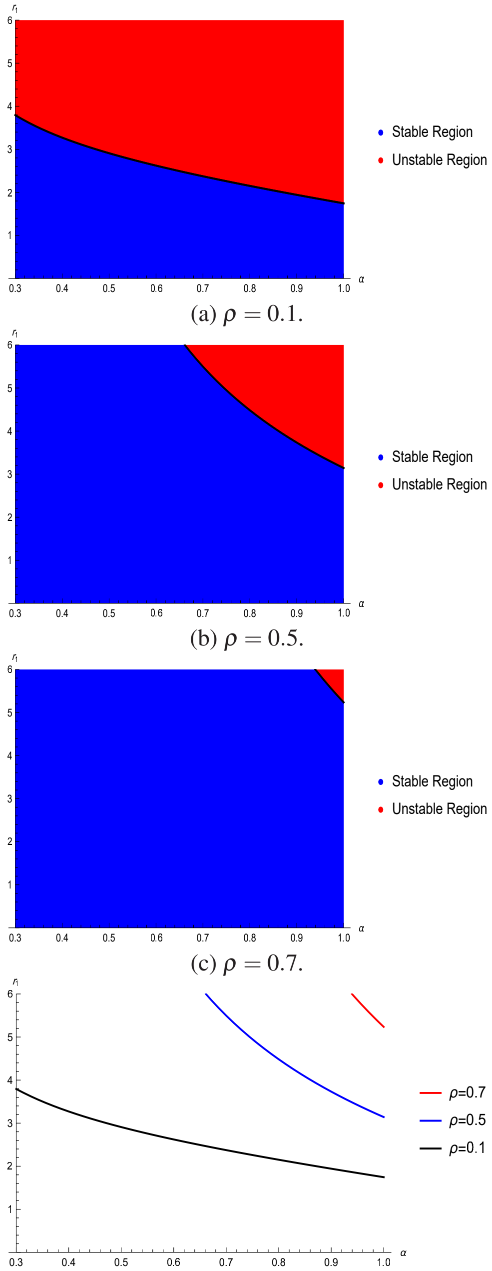

(a) $\rho = 0.1$. (b) $\rho = 0.5$. (c) $\rho = 0.7$. (d)

Fig. 3: Stability regions with respect to (α, r_1) when ρ varies from 0.1 to 0.7 and $\mu = 1$.

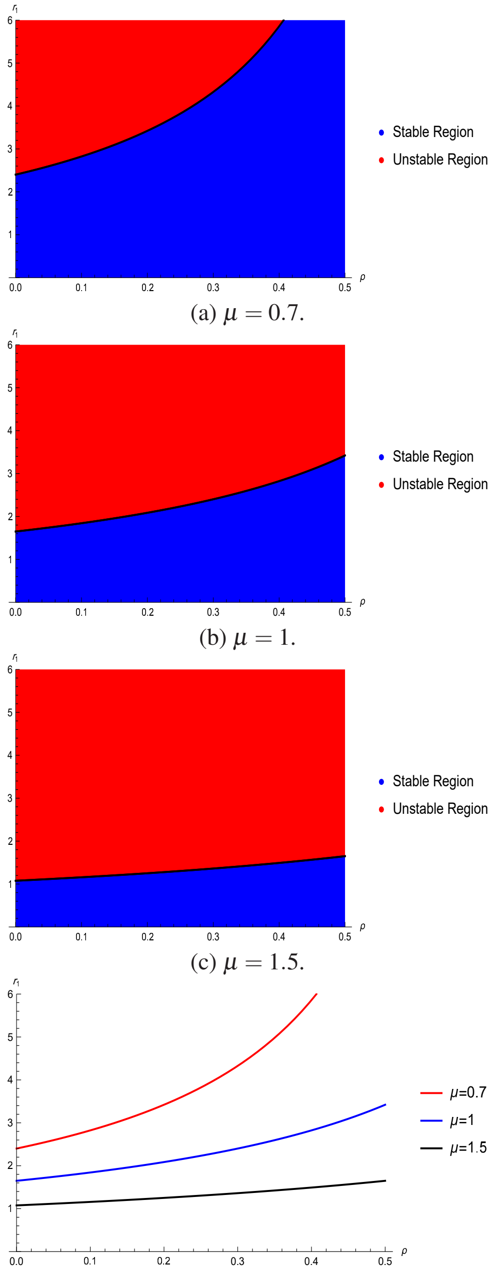

(a) $\mu = 0.7$. (b) $\mu = 1$. (c) $\mu = 1.5$. (d)

Fig. 4: Stability regions with respect to (ρ, r_1) when μ varies from 0.7 to 1.5 and $\alpha = 0.95$.

2.1.2 Stability for $y_2^* = -\frac{log\left(\frac{\mu}{\rho}\right)}{\gamma}$

From Eqs. (17) and (18), the critical curves for $y_2^* = -\frac{log\left(\frac{\mu}{\rho}\right)}{\gamma}$ are

$$r_1(n) = \frac{2n\pi + \pi(1-\alpha/2)}{\left(-\mu log\left(\frac{\mu}{\rho}\right)\right)^{\frac{1}{\alpha}}}, \quad n = 0, 1, \cdots. \tag{24}$$

and

$$r_2(n) = \frac{2n\pi - \pi(1-\alpha/2)}{\left(-\mu log\left(\frac{\mu}{\rho}\right)\right)^{\frac{1}{\alpha}}}. \quad n = 1, 2, \cdots. \tag{25}$$

We find that the critical curves are sensitive with the fractional order α, ρ and μ. See Fig. 6.

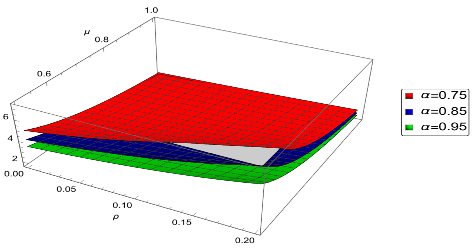

(a)

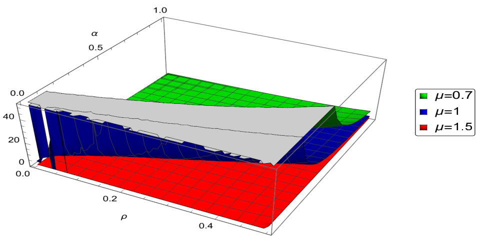

(b)

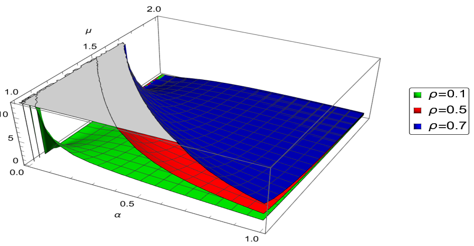

(c)

Fig. 5: Critical surfaces.

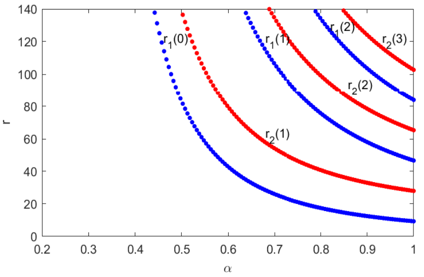

(a) $\rho = 0.7$, $\mu = 0.5$.

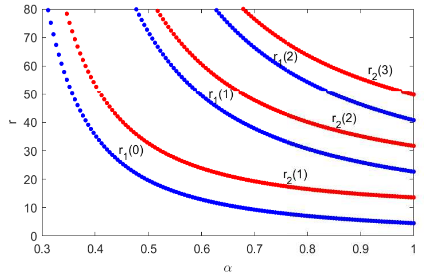

(b) $\rho = 1$, $\mu = 0.5$.

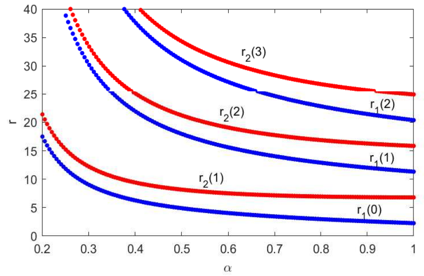

(c) $\rho = 2$, $\mu = 0.5$.

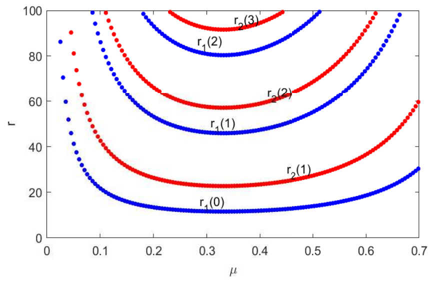

(d) $\alpha = 0.65$, $\rho = 0.9$.

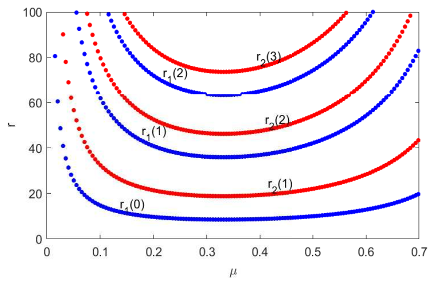

(e) $\alpha = 0.75$, $\rho = 0.9$.

Theorem 2.3. The equilibrium point $y_2^* = -\frac{log\left(\frac{\mu}{\rho}\right)}{\gamma}$ of Eq. (5) has only stability region located between $r = 0$ and

$$r_1(0) = \frac{\pi(1-\alpha/2)}{\left(-\mu log\left(\frac{\mu}{\rho}\right)\right)^{\frac{1}{\alpha}}}.$$

See Figs. 7-9.

We observe that the stability regions are sensitive with the fractional order α, μ, ρ and time delay. Stability regions with respect to μ, ρ, α and time delay are given in Figs. 7-9 and critical surfaces in Figs. 10. Figs. 7 and 8 show that the stability domain increases as the values of α and ρ decrease. Fig. 9 shows that the stability domain increases as the values of μ increase.

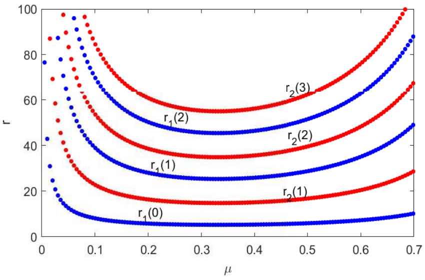

(f) $\alpha = 0.95$, $\rho = 0.9$.

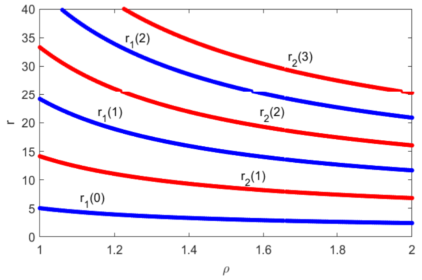

(g) $\mu = 0.5$, $\alpha = 0.95$.

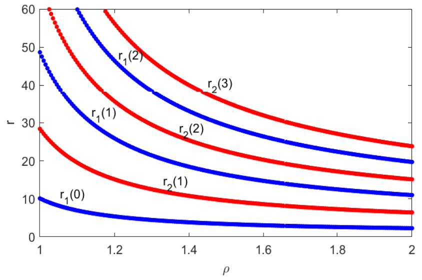

(h) $\mu = 0.8$, $\alpha = 0.95$.

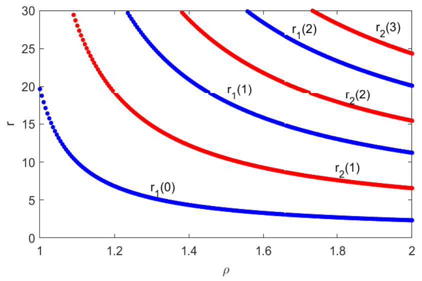

(i) $\mu = 0.9$, $\alpha = 0.95$.

Fig. 6: Critical curves of Eqs. (24) and (25).

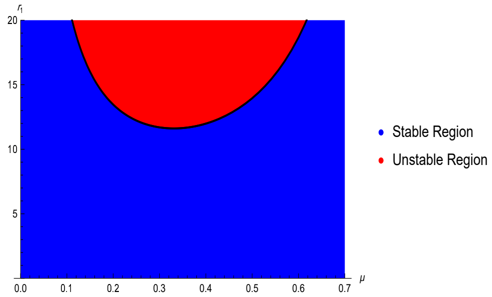

(a) $\alpha = 0.65$.

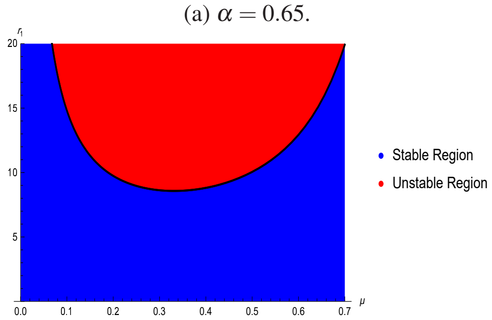

(b) $\alpha = 0.75$.

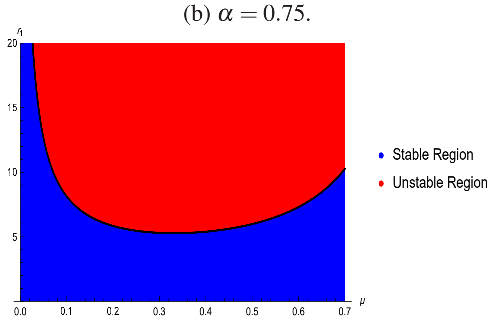

(c) $\alpha = 0.95$.

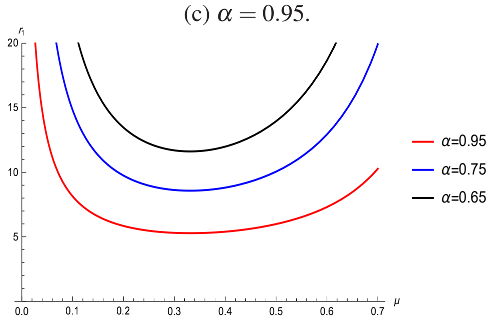

(d)

Fig. 7: Stability regions with respect to (μ, r_1) when α varies from 0.65 to 0.95 and $\rho = 0.9$.

2.2 Case 2: Dynamic analysis for two different delays $r_1 \neq r_2$

As in Sec.(2.1), we linearized Eq. (1) and get the characteristic equation of the form

$$\lambda^{\alpha} = -\mu e^{-\lambda r_1} + \rho e^{-\lambda r_2} (1 - \gamma y^*) e^{-\gamma y^*}. \tag{26}$$

At $\lambda = iv$, the characteristic equation becomes

$$(iv)^{\alpha} = -\mu e^{-ivr_1} + \rho e^{-\gamma y^*} (1 - \gamma y^*) e^{-ivr_2}. \tag{27}$$

Simplifying, we get

$$v^{\alpha} cos\left(\frac{\alpha\pi}{2}\right) + \mu cos(vr_1) = \rho e^{-\gamma y^*} (1 - \gamma y^*) cos(vr_2), \tag{28}$$

$$v^{\alpha} sin\left(\frac{\alpha\pi}{2}\right) - \mu sin(vr_1) = -\rho e^{-\gamma y^*} (1 - \gamma y^*) sin(vr_2). \tag{29}$$

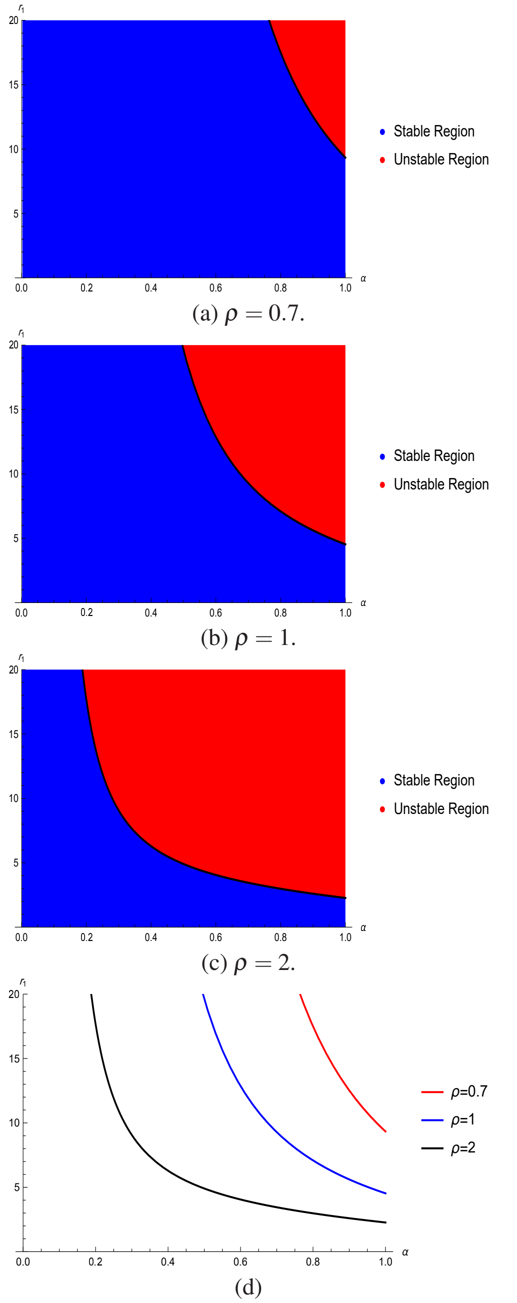

(a) $\rho = 0.7$.

(b) $\rho = 1$.

(c) $\rho = 2$.

(d)

Fig. 8: Stability regions with respect to (α, r_1) when ρ varies from 0.7 to 2 and $\mu = 0.5$.

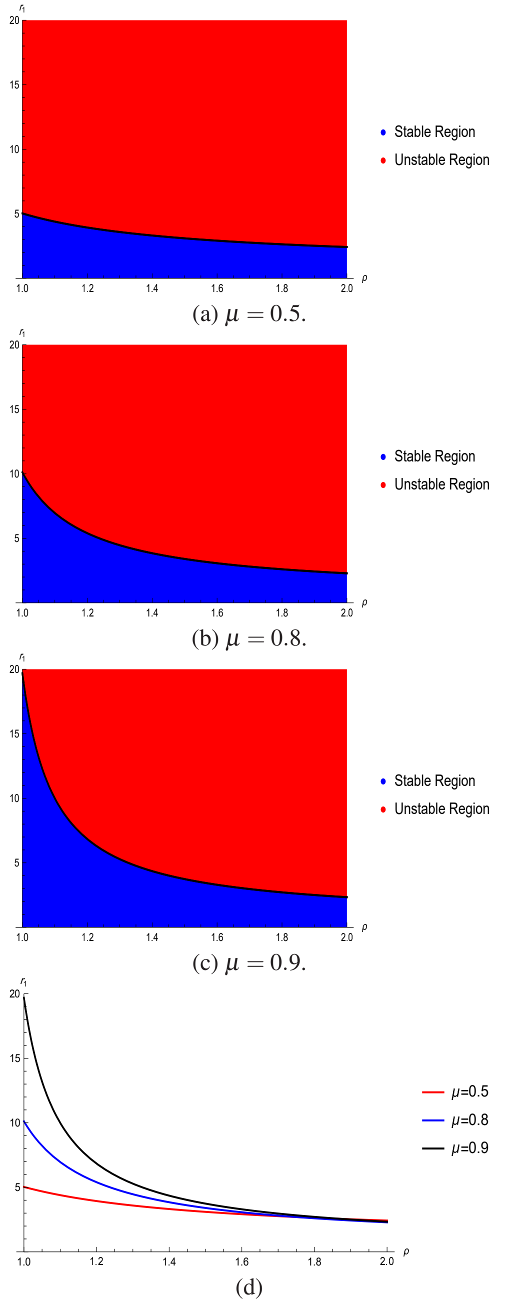

(a) $\mu = 0.5$.

(b) $\mu = 0.8$.

(c) $\mu = 0.9$.

(d)

Fig. 9: Stability regions with respect to (ρ, r_1) when μ varies from 0.5 to 0.9 and $\alpha = 0.95$.

Squaring and adding Eqs. (28) and (29), we get

$$v^{2\alpha} + \mu^2 + 2\mu v^{\alpha} cos\left(\frac{\alpha\pi}{2} + v r_1\right) = \rho^2 (1 - \gamma y^*)^2 e^{-2\gamma y^*} \tag{30}$$

From Eq. (30), we get the critical curves

$$r_1 = \frac{1}{v}\left(-\frac{\alpha\pi}{2} + arccos\left(\frac{v^{2\alpha} - \rho^2 e^{-2\gamma y^*}(1-\gamma y^*)^2 + \mu^2}{-2\mu v^{\alpha}}\right)\right), \tag{31}$$

and

$$r_2 = \frac{1}{v}\left(-\frac{\alpha\pi}{2} + arccos\left(\frac{v^{2\alpha} + \rho^2 (1-\gamma y^*)^2 e^{-2\gamma y^*} - \mu^2}{2 v^{\alpha} \rho e^{-\gamma y^*}(1-\gamma y^*)}\right)\right). \tag{32}$$

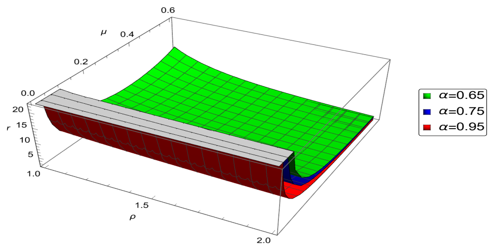

(a)

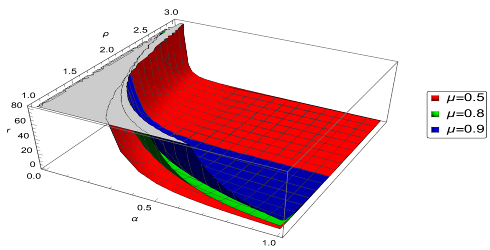

(b)

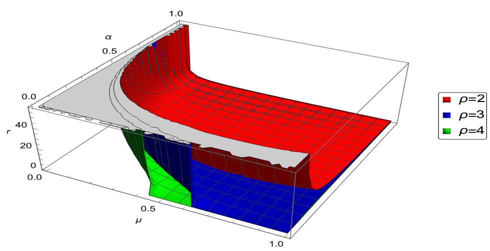

(c)

Fig. 10: Critical surfaces.

Fig. 11 shows that as the values of α become smaller, the stability domain becomes larger. Critical surfaces of Eqs. (31) and (32) are given in Fig. 12.

3 Numerical Simulations

An Adams-type predictor-corrector method has been introduced and investigated further in [26], [41,42,43,44,45,46]. In this section, we use an Adams-type predictor-corrector method for the numerical solution of the fractional integral equation.

The main problem is equivalent to the fractional integral equation

$$y(t) = y(0) + I^{\alpha}\left[-\mu y(t-r_1) + \rho y(t-r_2)e^{-\gamma y(t-r_2)}\right]. \tag{33}$$

and then apply the PECE (Predict, Evaluate, Correct, Evaluate) method.

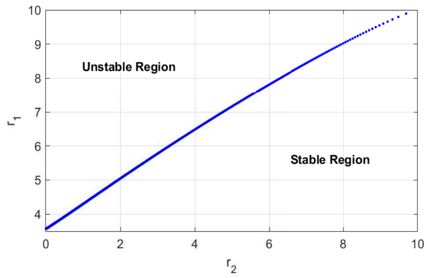

(a) $\alpha = 0.75$.

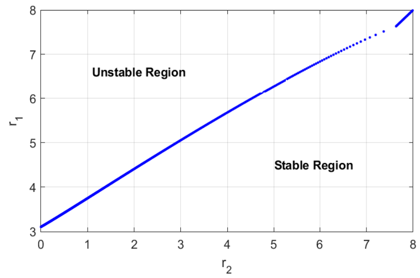

(b) $\alpha = 0.85$.

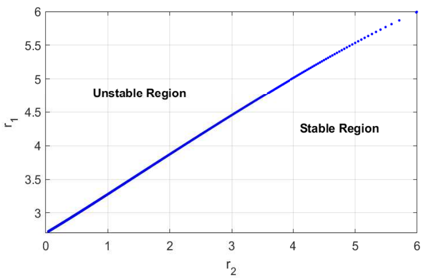

(c) $\alpha = 0.95$.

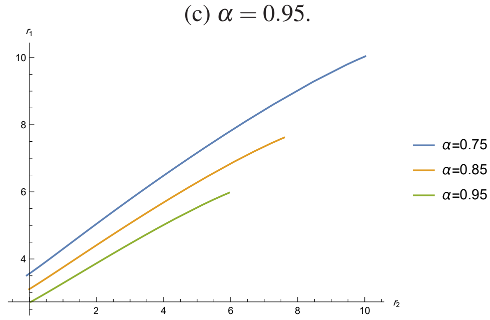

(d)

Fig. 11: Stability regions with respect to (r_2, r_1) when α varies from 0.75 to 0.95, $\mu = 0.5$, $\rho = 0.9$ and $\gamma = 0.5$.

3.1 Case 1: $r_1 = r_2 = r$

Fig. 13 for $r = 3$, $\alpha = 0.95$, $\rho = 0.1$ and different μ. Fig. 14 for $r = 6$, $\mu = 0.5$, $\rho = 0.1$ and different α. Fig. 15 for $\alpha = 0.95$, $\gamma = 0.5$, $\rho = 0.9$, $\mu = 0.5$ and different r. Fig. 16 for $r = 8$, $\gamma = 0.5$, $\rho = 0.9$, $\mu = 0.5$ and different α.

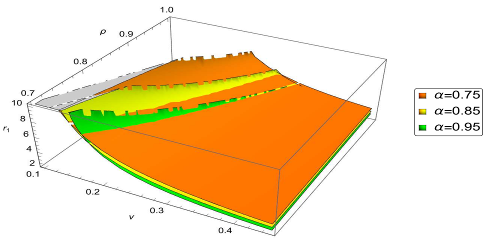

(a) $\mu = 0.5$.

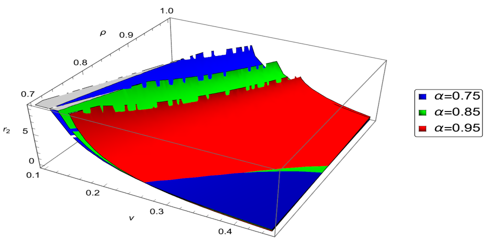

(b) $\mu = 0.5$.

Fig. 12: Critical surfaces of Eqs. (31) and (32) when α varies from 0.75 to 0.95 and $\gamma = 0.5$.

3.2 Case 2: $r_1 \neq r_2$

Fig. 17 for $\gamma = 0.5$, $\mu = 0.5$, $\rho = 0.9$ and $\alpha = 0.95$.

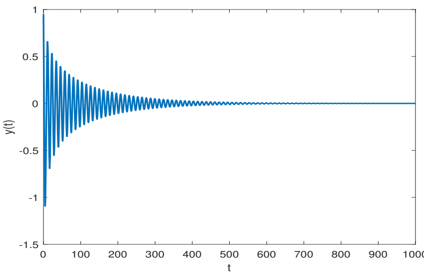

(a) $\mu = 0.65$.

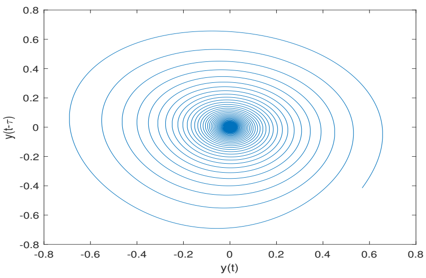

(b) $\mu = 0.65$.

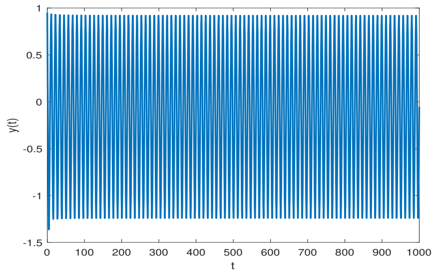

(c) $\mu = 0.75$.

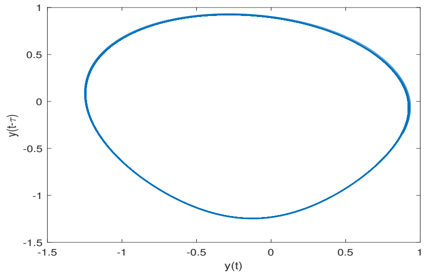

(d) $\mu = 0.75$.

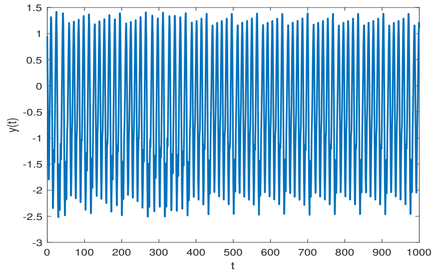

(e) $\mu = 0.91$.

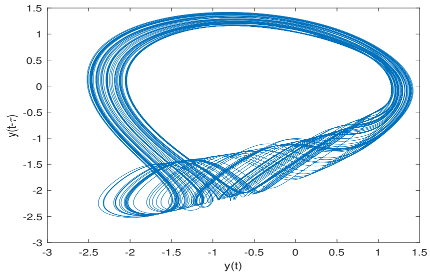

(f) $\mu = 0.91$.

Fig. 13: $r = 3$, $\alpha = 0.95$, $\rho = 0.1$ and μ varies from 0.65 to 0.91.

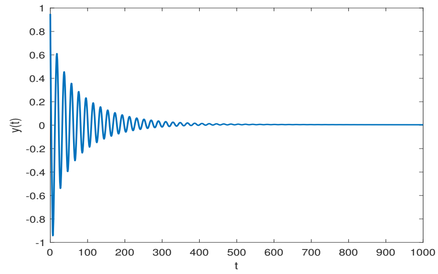

(a) $\alpha = 0.75$.

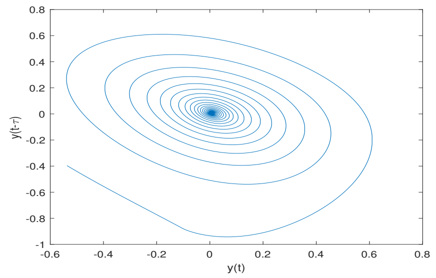

(b) $\alpha = 0.75$.

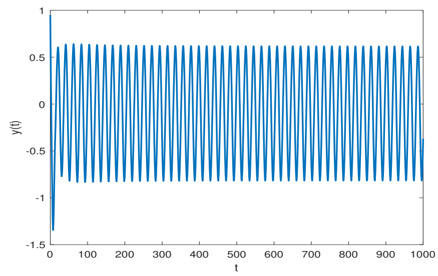

(c) $\alpha = 0.85$.

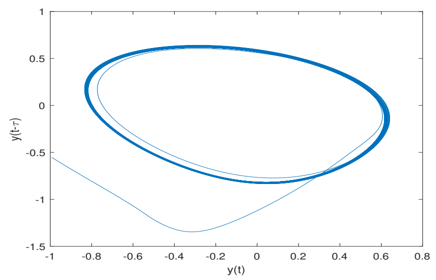

(d) $\alpha = 0.85$.

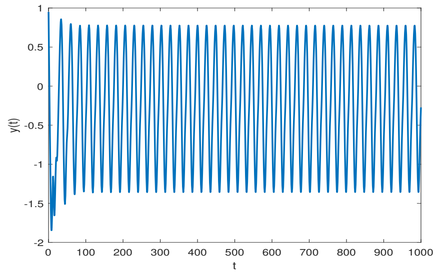

(e) $\alpha = 0.95$.

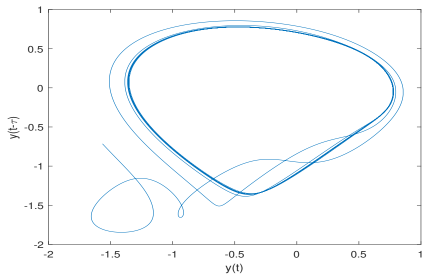

(f) $\alpha = 0.95$.

Fig. 14: $r = 6$, $\mu = 0.5$, $\rho = 0.1$ and α varies from 0.75 to 0.95.

4 Conclusions

In this paper, we have studied the dynamic analysis of a fractional-order Nicholson equation with two different delays. We discussed the stability and Hopf bifurcation for one delay $(r_1 = r_2 = r)$ and two different delays $(r_1 \neq r_2)$. According to the Theorems 2.2 and 2.3, we obtained the stability regions and critical curves for the equilibrium points y_1^* and y_2^*. We found that stability regions and critical curves are sensitive to the fractional order α, ρ, μ and time delay. Where we used μ, ρ, fractional order α and time delays as a bifurcation parameters. Also we obtained the critical surfaces for different ρ, μ, and fractional order α. We determined the parametric expressions of r_1 and r_2 and the stability regions between them for different fractional order α. Our results are confirmed by numerical simulations.

Funding
This research work is not supported by any funding agencies.

Conflicts of Interest
The authors declare that there are no conflicts of interest regarding the publication of this paper.

Acknowledgments
The authors would like to express their sincere thanks to the editor.

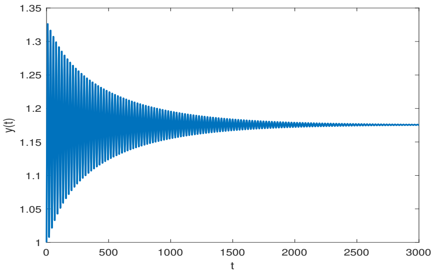

(a) $r = 5.9$.

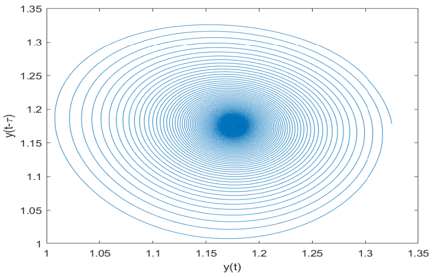

(b) $r = 5.9$.

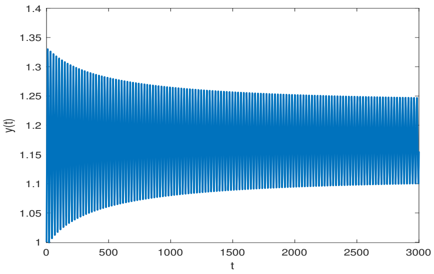

(c) $r = 6$.

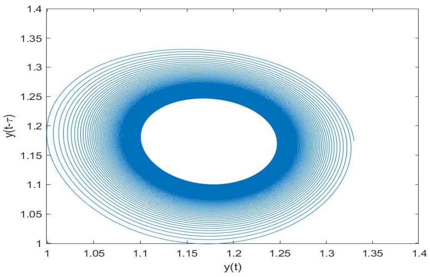

(d) $r = 6$.

Fig. 15: $\alpha = 0.95$, $\gamma = 0.5$, $\rho = 0.9$ and $\mu = 0.5$.

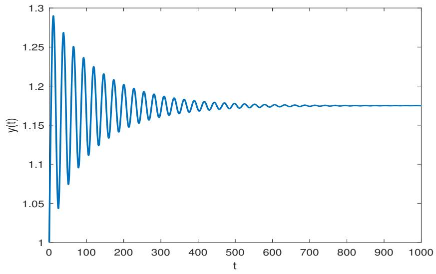

(a) $\alpha = 0.8$.

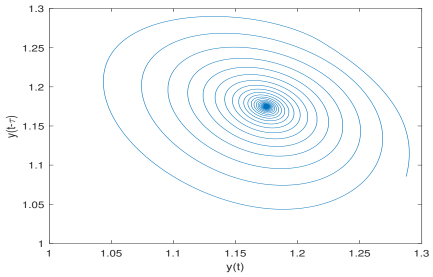

(b) $\alpha = 0.8$.

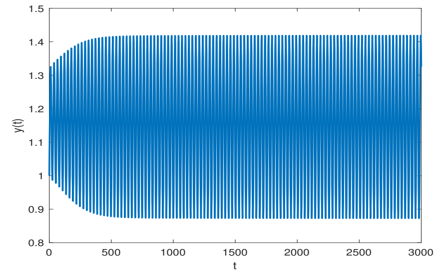

(c) $\alpha = 0.85$.

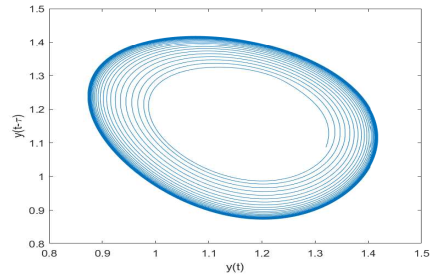

(d) $\alpha = 0.85$.

Fig. 16: $r = 8$, $\gamma = 0.5$, $\rho = 0.9$ and $\mu = 0.5$.

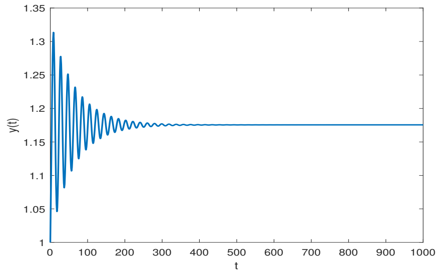

(a) $r_1 = 4.2$, $r_2 = 3$.

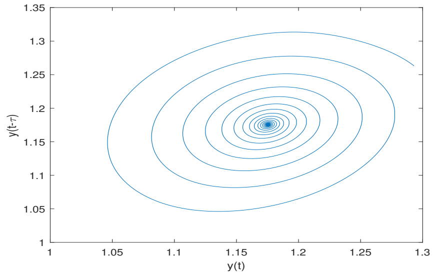

(b) $r_1 = 4.2$, $r_2 = 3$.

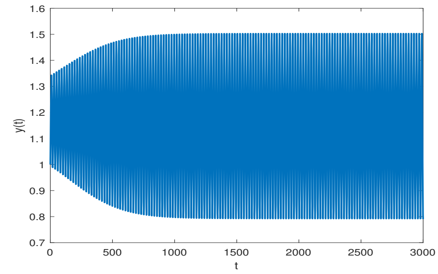

(c) $r_1 = 4.5$, $r_2 = 3$.

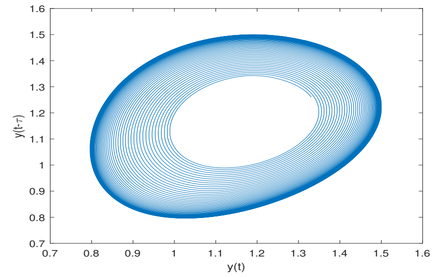

(d) $r_1 = 4.5$, $r_2 = 3$.

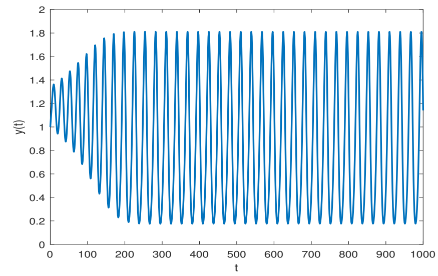

(e) $r_1 = 4.7$, $r_2 = 3$.

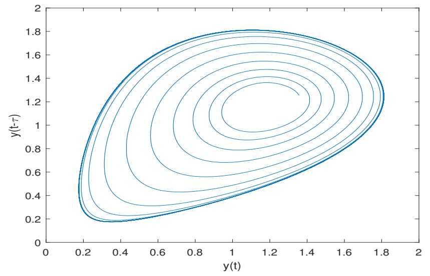

(f) $r_1 = 4.7$, $r_2 = 3$.

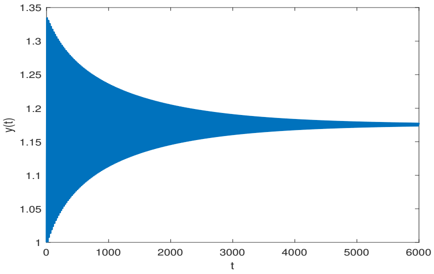

(g) $r_1 = 5$, $r_2 = 4$.

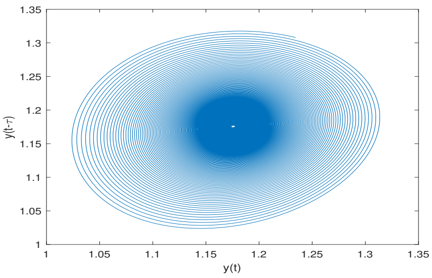

(h) $r_1 = 5$, $r_2 = 4$.

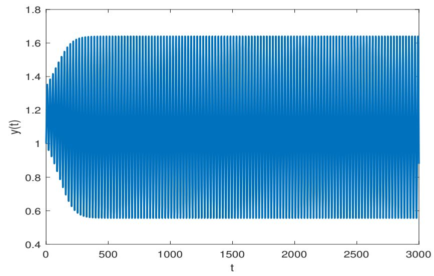

(i) $r_1 = 5.2$, $r_2 = 4$.

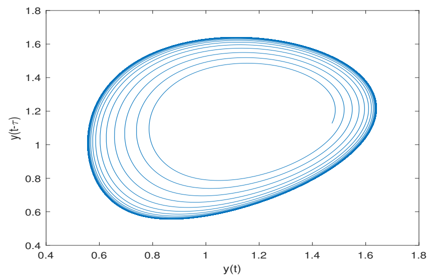

(j) $r_1 = 5.2$, $r_2 = 4$.

Fig. 17: $\gamma = 0.5$, $\mu = 0.5$, $\rho = 0.9$ and $\alpha = 0.95$.

References

[1] I. Podlubny, Fractional differential equations, Academic Press, 1999.
[2] L. Debnath, International Journal of Mathematics and Mathematical Sciences 2003, 3413-3442 (2003).
[3] H. Smith, An introduction to delay differential equations with applications to the life sciences, Volume 57, Springer New York, 2011.
[4] R. Hilfer, Applications of fractional calculus in physics, World scientific, 2000.
[5] H.A.A. El-Saka, S. Lee, J. Bongsoo, Nonlinear Dynamics 96, 407-416 (2019).
[6] A.M.A. El-Sayed, E. Ahmed, H.A.A. El-Saka, Abstract and Applied Analysis 2012, 251715 (2012).
[7] A.M.A. El-Sayed, F.M. Gaafar, Applied Mathematics and Computation 144, 117-126 (2003).
[8] CTH. Baker, GA. Bocharov, FA. Fathalla, University of Manchester, Manchester Centre of Computational Mathematics, Manchester, (1999).
[9] AC. Fowler, Journal of mathematical biology 13, 23-45 (1981).
[10] FA .Rihan, Delay differential equations and applications to biology, Springer, 2021.
[11] M. Lakshmana, D.V. Senthilkumar, Dynamics of nonlinear time-delay systems, Springer Science and Business Media, 2011
[12] R. Rakkiyappan, G. Velmurugan, F. Rihan, S. Lakshmanan, Complexity 21, 14-39 (2016).
[13] Y. Kuang, Delay differential equations: with applications in population dynamics, Academic press, 1993.
[14] GA. Bocharov, FA .Rihan, Journal of Computational and Applied Mathematics 125, 183-199 (2000).
[15] L. Berezansky, E. Braverman, Applied Mathematics and Computation 279, 154-169 (2016).
[16] X. Long, S. Gong, Applied Mathematics Letters 100, 106027 (2020).
[17] H.A.A. El-Saka, Mathematical Sciences Letters 2, 195 (2013).
[18] S. Bhalekar, V. Daftardar-Gejji,Communications in Nonlinear Science and Numerical Simulation 15, 2178-2191 (2010).
[19] Z. Wang, X. Huang, G. Shi, Computers and Mathematics with Applications 62, 1531-1539 (2011).
[20] H.A.A. El-Saka, A.A.M. Arafa, M.I. Gouda, Advances in Difference Equations 2019, 1-15 (2019).
[21] V. Feliu-Batlle, R. Rivas-perez, F.J. Castillo-Garcia, Computers and electronics in agriculture 69, 185-197 (2009).
[22] CA. Monje, Y. Chen, BM. Vinagre, D. Xue, V. Feliu-Batlle, Fractional-order systems and controls: fundamentals and applications, Springer Science and Business Media, 2010.
[23] H.A.A. El-Saka, I. Obaya, S. Lee, B. Jang, Scientific Reports 12, 20706 (2022).
[24] S. Bhalekar, Pramana 81, 215-224 (2013).
[25] S. Bhalekar, Chaos: An Interdisciplinary Journal of Nonlinear Science 26, (2016).
[26] E. Ahmed, A.M.A. El-Sayed, H. El-Saka, Journal of Mathematical Analysis and Applications 325, 542-553 (2007).
[27] A.M.A. El-Sayed, H.A.A El-Saka, E.M. El-Maghrabi, Zeitschrift für Naturforschung 66, 223-227 (2011).
[28] S. Bhalekar, Pramana 93, 1-7 (2019).
[29] WSC. Gurney, SP. Blythe, RM. Nisbet, Nature, 287, 17-21 (1980).
[30] A.M.A. El-Sayed, S.M. Salman, N.A. Elabad, Appl. Math. Sci 10, 503-518 (2016).
[31] T. Faria, H.C. Prates, Nonlinearity 35, 589 (2021).
[32] Y. Liu, J. Wei, Nonlinear Dynamics 105, 1805-1819 (2021).
[33] S. Panigrahi, S. Chand, Tatra Mountains Mathematical Publications 80, 135-144 (2021).
[34] M. Redha, S. Balamuralitharan, Advances in Difference Equations 2020, 1-20 (2020).
[35] V.P. Latha, F.A. Rihan, R. Rakkiyappan, G. Velmurugan, International Journal of Biomathematics 10, 1750111 (2017).
[36] I. Podlubny, A.M.A. El-Sayed, On two definitions of fractional calculus, Solvak Academy of science-institute of eyperimental phys, UEF-03-96 ISBN 80-7099-252-2, 1996.
[37] K. Diethelm, NJ. Ford, Lect. Notes Math 2004, 3-12 (2010).
[38] M. Ishteva, Department of Mathematics, University of Karlsruhe, Karlsruhe 5, (2005).
[39] A.M.A. El-Sayed, A.E.M. El-Mesiry, H.A.A. El-Saka, Applied Mathematics Letters 20, 817-823 (2007).
[40] M. Rakshana, P. Balasubramaniam, Neural Processing Letters, 1-19 (2023).
[41] K. Diethelm, Kai, AD. freed, Forschung und wissenschaftliches Rechnen 1999, 57-71 (1998).
[42] K. Diethelm, NJ. Ford, Hercma, 117-122 (2001).
[43] K. Diethelm, NJ. Ford, AD. Freed, Nonlinear Dynamics 29, 3-22 (2002).
[44] A.M.A. El-Sayed, A.E.M. El-Mesiry and H.A.A. EL-Saka, Computational & Applied Mathematics 23, 33-54 (2004).
[45] A.E.M. El-Mesiry, A.M.A. El-Sayed, H.A.A. El-Saka, Applied Mathematics and Computation 160, 683-699 (2005).
[46] A.M.A. El-Sayed, A.E.M. El-Mesiry, H.A.A. EL-Saka, International Journal of Modern Physics C: Computational Physics & Physical Computation 16, 1017-1025 (2005).

Hala El-Saka is a professor at the Department of Mathematics, Faulty of Science, Damietta University, Egypt.

Donia El-Sherbeny is a research student at the Department of Mathematics, Faculty of Science, Damietta University, Egypt.

Ahmed El-Sayed is a professor at Faculty of Science, Alexandria University, Egypt.